Korean J. Chem. Eng., **26**(3), 850-855 (2009)

Characterization, activity and selectivity of ethylenediamine modified Co/SiO$_2$ FT catalyst prepared by sol-gel method

Yuelun Wang*,, Bo Hou*, Jiangang Chen*, Litao Jia*, Debao Li*, and Yuhan Sun*,†**

*State Key Laboratory of Coal Conversion, Institute of Coal Chemistry, Chinese Academy of Sciences,
Taiyuan 030001, P. R. China
**Graduate School of Chinese Academy of Sciences, China

(*Received 16 July 2008 • accepted 23 December 2008*)

Abstract−Co/SiO$_2$ catalysts were prepared by sol-gel method with varied en (ethylenediamine)/Co molar ratios under the same pH. Their physical-chemical properties were compared with those prepared with similar en/Co molar ratios at natural pH or without adding ethylenediamine. Regardless of pH, the catalysts prepared using ethylenediamine possessed high microporosity, which led to a better selectivity to C$_{5-18}$ hydrocarbons, versus the catalyst possessing higher mesoporosity which showed slightly higher C$_{18+}$ selectivity. As enough positions in the coordination sphere were blocked by ethanediamine ligands, the formation of cobalt silicate disfavored for (en/Co=2) catalysts, which resulted in the higher activity in FT reaction. Whereas the catalysts prepared with lower or higher en/Co molar ratio both showed lower activity due to the formation of [(SiO)Co(en)(EtOH)$_3$] species or the electronic adsorption of cobalt complexes in the negatively charged silica surface, respectively. However, for the catalyst without using ethylenediamine, the lowest activity and the highest CH$_4$ selectivity obtained due to its much lower reducibility.

Key words: Cobalt Catalyst, Fischer-Tropsch Synthesis, Ethylenediamine, Sol-gel Method

INTRODUCTION

With the decrease of oil reserves and the tightness of fuel specifications, Fischer-Tropsch synthesis (FTS) has been attractive as one of the most promising pathways for the conversion of natural gas or coal to clean fuels and value-added chemicals via syngas. Cobalt-based FTS catalysts are usually preferred for the synthesis of long-chain paraffins, as they are more active per weight of metal, more stable toward deactivation by water, less active for the competing water-gas shift (WGS) reaction, and produce less oxygenates than the iron-based catalytic systems [1,2].

FTS with conventional supported metal catalysts usually yields a wide spectrum of hydrocarbons due to the Anderson-Schulz-Flory (ASF) polymerization kinetics [3]. It imposes a limitation on the maximum selectivity for a given hydrocarbon product, such as C$_5$-C$_{18}$ paraffins (middle distillates) [4]. To get around such a barrier, structure-controlled cobalt catalysts were investigated to realize the selective FT synthesis for the middle distillates. For instance, Tsubaki et al. synthesized H-ZSM-5 zeolite membranes on the Co/SiO$_2$ catalysts, and excellent selectivity on the middle isoparaffins was observed over these catalysts benefiting from the confined reaction conditions constructed by zeolite capsules [5]. Liu et al. found that cobalt catalysts supported on mesoporous zirconia displayed higher selectivity to C$_{12}$-C$_{18}$ paraffin in FTS due to ordered porous structures of mesoporous molecular sieves with control of product distributions [6]. Mochizuki et al. have recently found that Co/SiO$_2$ catalysts prepared from an impregnating solution containing both Co nitrate and nitrilotriacetic acid (NTA) exhibited 3 times greater space time yield (STY) of C$_{10}$-C$_{20}$ hydrocarbon than that of the catalyst prepared without chelating agents in FTS [7].

In addition, Edward et al. observed that Co/SiO$_2$ catalysts prepared by sol-gel method could also favor synthesis of diesel range hydrocarbons via tuning the porosity of catalysts [8]. Ernst et al. [9] synthesized Co/SiO$_2$ catalysts by pseudo sol-gel technique and found that catalysts showed a better selectivity to C$_5$-C$_{13}$ fraction in FTS. Recently, in our group, sol-gel derived Co/SiO$_2$ catalysts were prepared with the modification of chelating agent (en). A higher selectivity to C$_5$-C$_{18}$ hydrocarbons (middle distillates) was observed over these catalysts [10]. However, the effect of ethylenediamine has not been clearly understood. It was suggested that both the coordination process and the pH of the solution were responsible for the final reducibility of Co species, pore structures and concomitant catalytic performances of those catalysts. To further investigate the influence of synthesis parameters on such sol-gel systems, especially the coordination process between ethylenediamine and cobalt ions, Co/SiO$_2$ catalysts were prepared by the sol-gel method via adding different amounts of ethylenediamine, and then nitric acid was used to adjust the pH value ensuring that all the preparation processes were performed under the same pH.

EXPERIMENTAL

1. Catalysts Preparation

Tetraethoxysilane (TEOS), cobalt nitrate were dissolved in alcohol with a composition of 15 wt%Co in SiO$_2$, and then ethylenediamine was added with the molar ratio of en/Co equaled to 1, 2, and 3.75, respectively. A certain amount of water was added. Nitric acid was added dropwise into the solution of en/Co molar ratio of 2 and 3.75 so that their pH values were closed to that of 1en-Cat (pH~

[†] To whom correspondence should be addressed.
E-mail: yhsun@sxicc.ac.cn

[‡] This work was presented at the 7th China-Korea Workshop on Clean Energy Technology held at Taiyuan, Shanxi, China, June 26-28, 2008.

4.4). Then catalysts were stirred for 24 h, dried at 333 K and calcined in air at 673 K for 6 h. Catalysts were denominated as 1en-Cat, 2en-N and 3.75en-N according to the molar ratio of en/Co. For a reference, Co/SiO_2 catalysts with the molar ratio of en/Co equaled to 0, 2 and 3.75 without control of pH were also synthesized. They were denoted as 0en-Cat, 2en-Cat and 3.75en-Cat.

2. Catalyst Characterization

Diffuse reflectance UV-vis spectra of catalyst precursors were obtained at ambient conditions with a Varian-Cary 4 spectrophotometer with $BaSO_4$ as a reference. The surface area and pore characteristics of catalysts were determined by nitrogen adsorption/desorption measurements using a Micromeritics Tristar 3000 sorptometer at 77 K. The thermogravimetric analyses were performed on a Setaram 92-12 thermogravimeter. The sample was placed into air flow in an alumina crucible and the temperature was increased with a 1 K min^{-1} slope from 298 to 873 K. X-ray diffraction (XRD) patterns of the samples were recorded on a Bruker B5005 diffractometer using Cu Ka radiation. The mean Co_3O_4 crystallite sizes were estimated from the XRD data by using the Scherrer equation. TPR was performed in a U-tube quartz reactor at the ramp rate of 10 K/min in the 5% H_2/Ar (vol.) flow of 30 ml/min. The H_2 consumption was monitored with TCD by using the reduction of CuO as the standard. The reduction percentage of the cobalt oxides at temperatures less than 673 K was calculated from the TPR profiles.

3. Catalytic Experiments

Catalysts were evaluated in a pressured fixed-bed reactor at 2 M Pa, 1,200 h^{-1} with the H_2/CO ratio of 2 after reduction at 673 K for 10 h. Wax was collected with a hot trap and the liquid products were collected in a cold trap. The gas effluents were analyzed on-line by using a Carbosieve-packed column with TCD. The gas hydrocarbons were analyzed on-line using Porapak-Q column with FID. Oil and wax were analyzed offline in OV-101 capillary columns. 5% N_2 was added to syngas as an internal standard. The carbon balance and mass balance were 100±5%.

RESULTS AND DISCUSSION

1. The Sol-gel Processing of Catalyst Precursors

To monitor the evolution of cobalt species during the sol-gel process, the precursors, gel of catalysts were characterized with XRD, UV-vis spectra and TGA.

The XRD patterns of precursors, dried gel of catalysts are shown in Fig. 1. The typical diffraction peaks of $[Co(en)_3](NO_3)_2$ (JCPDS file number 50-1926) appeared over 2en-Cat and 3.75en-Cat without control of pH. But the samples prepared without ethanediamine or one ethanediamine per Co showed much weaker diffraction peaks due to the formation of ill-crystallized species. And $[Co(en)_3](NO_3)_2$ seemed to be the unique crystallized phase. The diffraction peaks increased with the increasing amount of ethylenediamine, indicating the improvement of the crystal perfection of $[Co(en)_3](NO_3)_2$. With the addition of nitric acid, the diffraction peaks for 2en-N and 3.75en-N changed slightly. It was suggested that there might be new crystallized phases formed. However, unfortunately, it was difficult to assign these peaks as probably several species coexisted. Especially, the comparison between JCPDS file 50-1926 and ref. [11] showed that the diffraction peaks of Co(II) and Co(III) salts came out at the same values due to their similar unit cell parameters. Thus, both Co(II)-en complexes and Co(III)-en complexes oxidized from Co(II)-en complexes possibly co-existed in these cobalt precursors. Compared with the diffraction peak of cobalt nitrate hexahydrate, it was obvious that ligand transformation had taken place for catalysts with the addition of ethylenediamine.

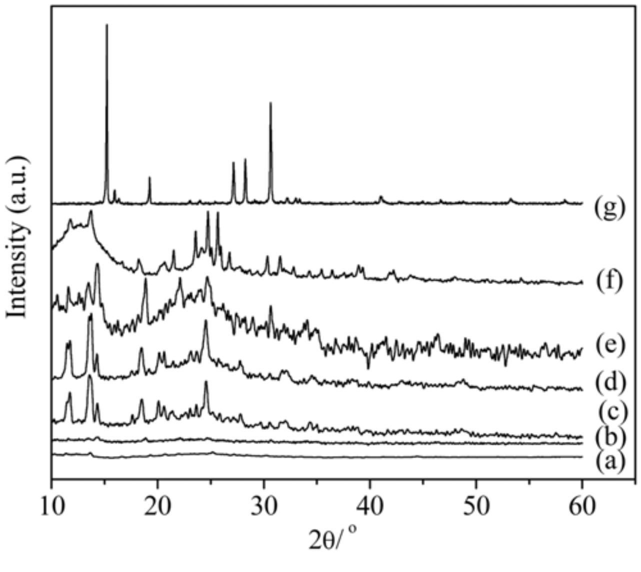

Fig. 1. XRD of dried sol-gel cobalt catalysts. (a) 0en-Cat (b) 1en-C (c) 2en-C (d) 3.75en-C (e) 2en-N (f) 3.75en-N (g) $Co(NO_3)_2$·$6H_2O$.

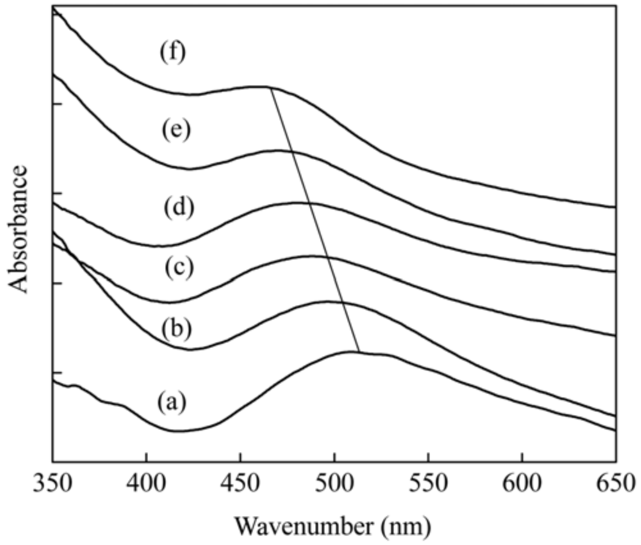

Fig. 2. UV-visible spectra of dried sol-gel cobalt catalysts. (a) Co$(NO_3)_2$·$6H_2O$ (b) 1en-Cat (c) 2en-Cat (d) 3.75en-Cat (e) 2en-N (f) 3.75en-N.

The UV-vis spectra of catalyst precursors are shown in Fig. 2. The absorption of cobalt (II) nitrate hexhydrate appeared at 515 nm. With the addition of ethylenediamine, the absorption band shifted to lower wavenumbers, implying the significant modification of local coordination of cobalt. The absorption band around 505 nm for 1en-Cat was mainly attributed to the complex $[Co(en)(EtOH)_4](NO_3)_2$. However, the absorption bands at 489 nm and 478 nm appeared for 2en-Cat and 3.75en-Cat. These bands originated from Co(II)-en complexes [12]. Referring to the stability constants of Co(II)-en complexes ($\log\beta i$=5.4, 10.2 and 13.8) [13], $[Co(en)_2](NO_3)_2$ with a portion of $[Co(en)_3](NO_3)_2$ was expected for the Co/en molar ratio of 2/1, and $[Co(en)_3](NO_3)_2$ was expected with the en/Co molar ratio up to 3.75. Moreover, with the addition of nitric acid, the absorption band further shifted to lower wavenumbers, which were observed at 471 nm and 466 nm for 2en-N and 3.75en-N, respectively. The shift of absorption band was ascribed to the formation of Co(III) complexes [11], such as, $[Co(en)_2](NO_3)_3$ mainly for 2en-N, $[Co(en)_3](NO_3)_3$ for 3.75en-N. However, it should be noted that nitric acid was just dropwise added to adjust the pH value; thus only a part of Co(II)-en complexes were oxidized and quite a large quantity of $[Co(en)_2]$ $(NO_3)_2$ and $[Co(en)_3](NO_3)_2$ still remained.

TGA of the dried catalysts is given in Fig. 3, which shows that all catalysts had completely decomposed before the chosen calcination temperature (673 K). The first weight loss, which was attributed to the removal of physisorbed water and alcohol, occurred below 393 K. The second large weight loss, between 423 and 484 K, was ascribed to the decomposition of $[Co(EtOH)_6](NO_3)_2$. This step was only observed on the 1en-Cat. The third weight loss with multiple decomposition peaks was observed between 486 and 620 K. It might be involved in a complicated process. These multiple peaks were attributed to the several phases coexisting in the system, which were observed more evidently for the 1en-Cat. As observed, the weight loss did not match with the amount of ethylenediamine in the TGA data. That is, with increasing the amount of ethylenediamine in catalysts, the amount of weight loss did not increase. It could well be explained by the formation of different species involving cobalt complexes and cobalt-silica interaction species. Besides cobalt complexes, the formation of cobalt-silica interaction species, such as, grafted complex $[(SiO)Co(en)(EtOH)_3]$, also contributed to the multiple decomposition peaks. For 1en-Cat and 3.75en-N samples, the formation of cobalt-silica interaction species was favored, which was witnessed in the following TPR profiles. Whereas, the presence of two ethanediamine ligands per Co inhibited the formation of cobalt-silica interaction species. Thus, its weight loss mainly corresponded to the decomposition of cobalt complexes on 2en-N sample. As a consequence, the order of the weight loss was 1en-Cat> 3.75en-N>2en-N catalysts.

2. Physico-chemical Properties of Catalysts

Fig. 4 displays XRD patterns of calcined catalysts. All catalysts show the characteristic peaks of Co_3O_4 species at 36.7°. The intensity of spectra increased gradually with the increasing amount of ethylenediamine. Average crystal sizes of Co_3O_4 particles were calculated by Scherrer equation [14] (see Table 1). Clearly, the sizes of Co_3O_4 crystallites increased with the increasing amount of ethylenediamine. Whereas, larger Co_3O_4 particle sizes were obtained over those catalysts prepared under control of pH. The largest Co_3O_4 particles presented over 0en-Cat.

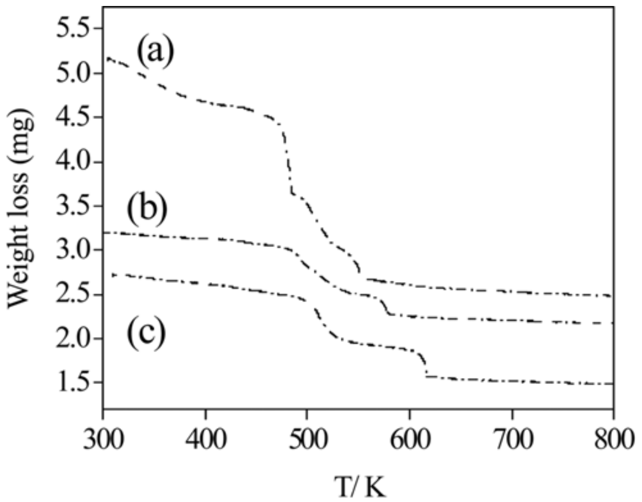

Fig. 3. TGA of dried sol-gel cobalt catalysts. (a) 1en-Cat (b) 2en-N (c) 3.75en-N.

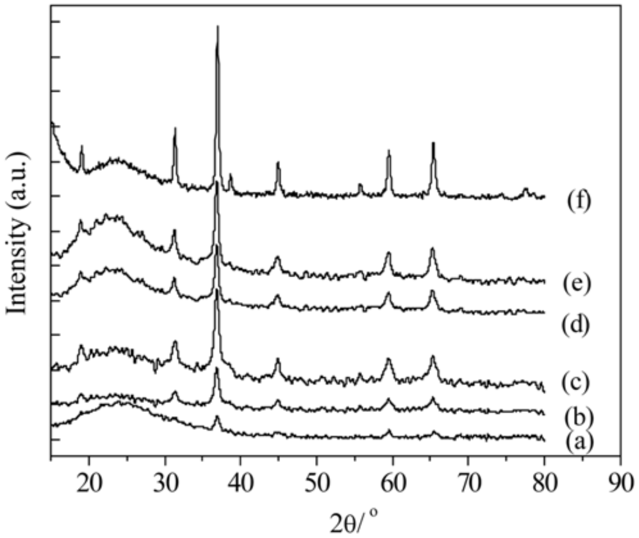

Fig. 4. XRD of cobalt catalysts. (a) 1en-Cat (b) 2en-Cat (c) 3.75en-Cat (d) 2en-N (e) 3.75en-N (f) 0en-Cat.

Table 1. Texture and phase structure properties of cobalt catalysts

Catalyst	BET surface (m^2/g)	Pore size (nm)	Pore volume (cm^3/g)	Micro./total pore volume (%)	Particle size of Co_3O_4 (nm)	Reducibility of catalysts (%)
0en-Cat	27	14.3	0.05	5.0	19.8	22.6
1en-Cat	292	2.5	0.17	57.0	7.0	49.1
2en-Cat	154	10.9	0.42	12.0	12.5	91.7
3.75en-Cat	221	4.2	0.21	25.0	13.4	56.6
2en-N	227	3.2	0.18	48.0	15.8	85.2
3.75en-N	242	5.5	0.33	23.0	16.9	54.3

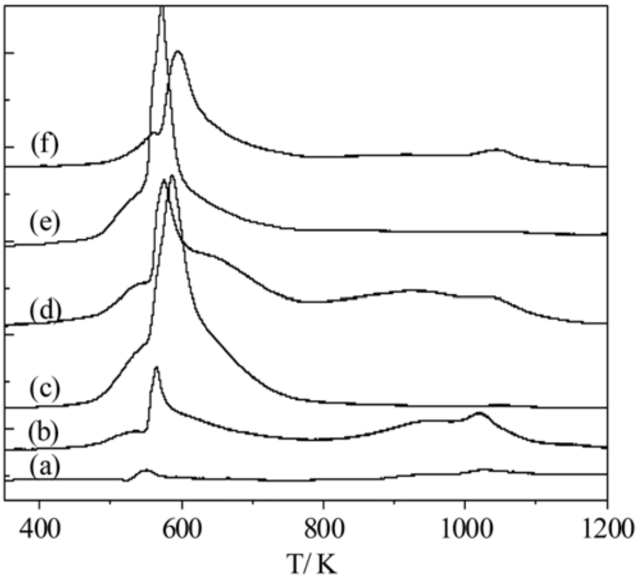

Fig. 5. TPR of cobalt catalysts. (a) 0en-Cat (b) 1en-Cat (c) 2en-Cat (d) 3.75en-Cat (e) 2en-N (f) 3.75en-N.

Table 2. Catalytic performance of cobalt catalysts in FT synthesis

Catalyst	CO conversion/%	C_1/%	C_{2-4}/%	C_{5-18}/%	C_{18+}/%
0en-Cat	14.2	22.4	4.7	63.7	9.2
1en-Cat	64.2	15.4	4.2	74.2	6.2
2en-Cat	95.3	20.2	5.2	62.8	11.8
3.75en-Cat	76.8	19.8	5.6	68.2	6.4
2en-N	83.4	19.6	5.3	67.2	7.8
3.75en-N	71.2	18.7	4.3	70.2	6.8

Reaction conditions: T=503 K, H_2/CO=2, GHSV=1,200 h^{-1}, P=2 Mpa

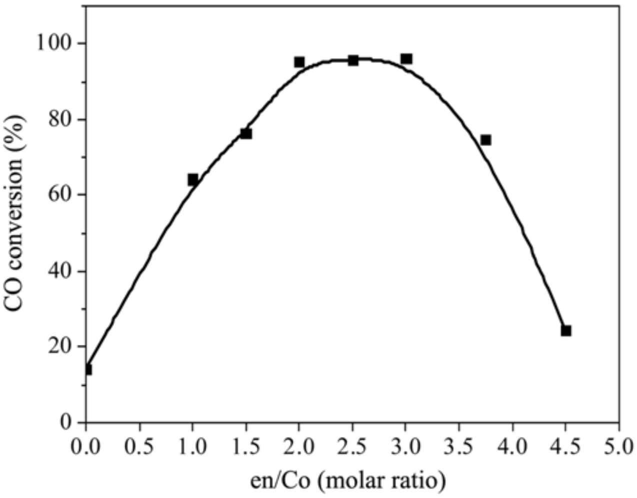

Fig. 6. Relationship between the CO conversions and the en/Co molar ratios for cobalt catalysts.

Table 1 shows the textural properties of the calcined catalysts. The surface areas varied between 27 and 292 m^2/g along with different pore sizes. Except for 0en-Cat and 2en-Cat, smaller pore sizes were observed over these catalysts; moreover, a large portion of micropore volume presented (see Table 1). In the case of 0en-Cat and 2en-Cat, much larger pore sizes were obtained. Especially, for 0en-Cat catalyst, much lower surface area was observed compared to other catalysts prepared with the modification of ethylenediamine. It is obvious that both ethylenediamine and pH had strong influence on the pore structure.

The TPR profiles of the catalysts are shown in Fig. 5. The reduction behavior was significantly related to the amount of ethylenediamine. The peaks at 473-673 K were attributed to the reduction of bulk Co_3O_4 ($Co^{3+} \rightarrow Co^{2+} \rightarrow Co^0$) [15], and the high temperature peak (673-1,073 K) was attributed to the reduction of cobalt oxide and silica interaction species [16]. The disappearance of high-temperature reduction peaks for 2en-serial catalysts implied the easier reduction due to the weaker cobalt-silica interaction. Stronger interaction was observed on the other catalysts, as higher reduction temperature for cobalt silicates appeared in those samples. The broad reduction process at 773-1,073 K for 1en-Cat and 3.75en-Cat seemed to comprise more than one peak indicating the different interaction degrees between cobalt and silica. The reduction degrees of catalysts are listed in Table 1. 2en-Cat showed the highest reducibility, and 0en-Cat had the lowest reducibility due to the strong cobalt-silica interaction.

3. Catalytic Performances in FTS

The FTS catalytic results are summarized in Table 2. Under the same reaction temperature (503 K), 2en-N catalyst displayed a much higher CO conversion than that of others. The order of CO conversion was 2en-N>3.75en-N>1en-cat. The results are consistent with the previous results over the catalysts prepared without control of pH. That is, the highest FTS activity was observed for catalysts with the en/Co molar ratio of 2/1, while the catalysts with lower or higher en/Co molar ratios showed negative effects. Thus, the en/Co molar ratio played an important role in determining the final catalytic properties. To get more information about the relationship between FTS activity and en/Co molar ratios, a series of catalysts with varied en/Co molar ratios were prepared at natural pH. In Fig. 6, the steady-state CO conversions over reduced catalysts at 673 K are plotted against en/Co molar ratios. An appropriate en/Co molar ratio was important for obtaining the higher FTS activity. Such a similar volcano-type dependency was also observed by Mochizuki et al. They found that the maximum conversion was obtained with the catalyst prepared with the chelating agent having an intermediate complex formation constant, i.e., nitrilotriacetic acid (NTA). Whereas, the complexes having much smaller or larger complex formation constants showed negligible or negative effects [17]. But a further investigation was not given. Trujillano et al. [18] studied the speciation of cobalt ethanediamine (en) complexes supported on silica. They found that the presence of two ethanediamine ligands per Co could inhibit the formation of cobalt silicate due to the block of the coordination sphere by inert ethanediamine ligands. Related with our work, the main species $[Co(en)_2((EtOH)_2)]$ on (en/Co=2) samples should have an initial lower interaction with the support. A large quantity of cobalt oxide was therefore obtained on calcined 2en-series. That allowed the higher reducibility and a concomitant higher FTS activity. While the en/Co molar ratio was 1/1, the presence of one ethanediamine ligand per Co ((en/Co=1) sample) favored the formation of $[(SiO)Co(en)(EtOH)_3]$ species that decomposed into cobalt silicate after calcinations. However, for (en/Co=3.75) sam-

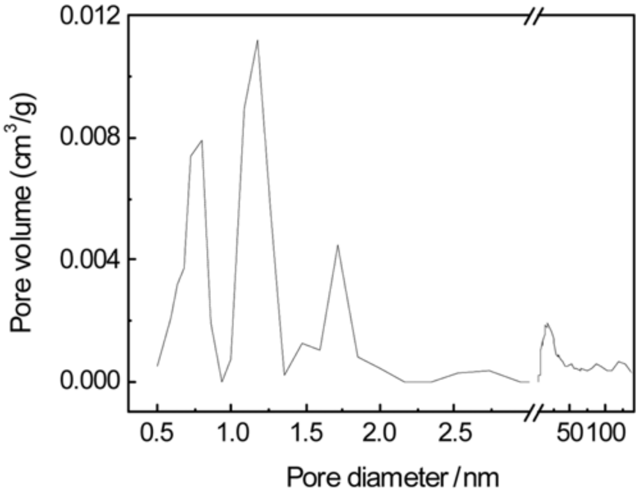

Fig. 7. Pore size distribution cures of the sample (1en-Cat).

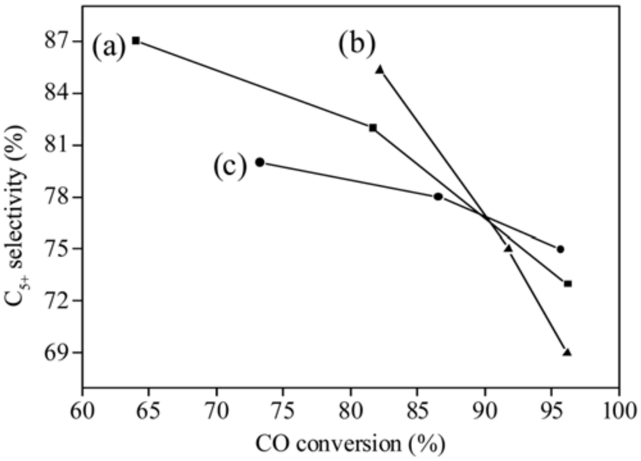

Fig. 8. Changes of C_{5+} selectivity versus CO conversion for catalysts. (a) 1en-Cat (b) 2en-N (c) 3.75en-N.

ples, the enhanced cobalt-silica interaction still took place. We thought that the electrostatic adsorption would account better for our observations. A portion of free ethylenediamine resulted in the negatively charged silica-gel surface, which could strongly adsorb cobalt complexes, and then lead to stronger cobalt-silica interaction. Obviously, lower reducibility was obtained for (en/Co=1, 3.75) samples, as well as lower activity was observed.

On the other hand, distinct hydrocarbon selectivities were found for the different catalysts. The highest CH_4 selectivity was observed for 0en-Cat. The other catalysts showed higher selectivity to C_{5-18} hydrocarbons. In addition, a slightly higher C_{18+} selectivity was also observed for 2en-Cat. Changes in the product array could be attributed to the different physical-chemical properties of catalysts. For those catalysts possessing a large proportion of microporosity (see Fig. 7 and Table 1), the diffusion rate of reactants and products became slower in micropore channels; accordingly, C_{5-18} hydrocarbons as the main compounds were observed. While for 2en-Cat with lower portion of microporosity, a slightly higher C_{18+} selectivity was observed, which resulted from the less diffusion limitation in larger pores favoring the formation of longer hydrocarbon chains. However, despite the decrease of microporosity, C_{5-18} fraction did not tend to decrease, since the FT reaction was comprised of a large number of elementary steps, such as dissociation, hydrogenation, and insertion. Therefore, the production of hydrocarbons was a complicated process. It could be expected that many factors, such as pore structures, the morphology of metal particles, the location and the number of active sites etc., could affect the final selectivity of FT synthesis. For instance, 0en-Cat had larger pore size, but much smaller surface area was presented; thus the active Co sites exposed on the reduced catalyst surface were much lower, reasonably allowing the lowest reducibility and concomitant lower catalytic activity and higher CH_4 selectivity. The higher methane selectivity might thus be responsible for its low C_{5+} selectivity. From the above, it was concluded that both pore structure of catalysts and Co^0 active sites could affect the product selectivities. For those ethylenediamine-modified catalysts, the pore structure was the main influence factor, while the reducibility mainly determined the selectivity of 0en-Cat.

In addition, it is well known that FTS selectivities may be affected by conversion, and they should be compared at similar conversion levels to assess any changes arising from differences in catalyst properties. Therefore, the relationship between C_{5+} selectivities and CO conversion among these catalysts was plotted (see Fig. 8). For all the catalysts, the C_{5+} selectivity decreased with decreasing CO conversion. As the catalysts displayed the very close CO conversion levels (about 90%), catalysts showed the same C_{5+} selectivity. But, at the higher or lower CO conversion, the different change for C_{5+} selectivity versus CO conversion presented on these catalysts. At lower CO conversion level, a strong dependence on reducibility for C_{5+} selectivity was observed. The highest C_{5+} selectivity was observed on 2en-N due to its highest reducibility, suggesting that not only pore structure of catalysts but also Co^0 active sites could affect the product selectivities. A higher concentration of Co^0 active sites usually favored chain growth. However, the opposite trend for product selectivity was observed at higher CO conversion level. 2en-N showed the highest methane selectivity. Anderson et al. [19] attributed the observed increase in methane selectivity to mass transport phenomenon. It was suggested that a greater rate of diffusion of hydrogen compared to that of carbon monoxide inside pores filled with liquid products caused an increase in H_2/CO ratio in catalyst pores, and thus, a shift toward formation of lighter hydrocarbons. In the present work, the higher concentration of Co^0 active sites probably favored the greater rate of diffusion of hydrogen under the higher CO conversion. Thus, higher CH_4 selectivity was observed for 2en-N. On the contrary, 1en-Cat and 3.75en-N with concentration of Co^0 active sites showed more stable and higher C_{5+} selectivity. However, the catalysts with the highest reducibility showed increasing methanation rate at higher CO conversion level; thus the lowest C_{5+} selectivity was observed.

CONCLUSION

Cobalt catalysts were prepared with a modified sol-gel method by controlling ethylenediamine amounts under the same pH. Catalysts prepared with the modification of ethylenediamine under acid medium possessed a large fraction of microporosity, which led to a better selectivity to C_{5-18} fraction. However, the catalyst prepared with en/Co molar ratio of 2/1 showed higher methane selectivity at the higher CO conversion level due to an increase of H_2/CO ratio; on the contrary, the catalysts prepared with en/Co molar ratios of 1 or 3.75 were of more stable and higher C_{5+} selectivity. The results also showed that the catalytic activities were greatly related to the en/Co molar ratio rather than pH value. The highest CO conversion was observed on the catalyst prepared with the molar ratio en/Co of 2/1, which originated from the Co-en complexes with the weaker cobalt-silica interaction resulting in higher reducibility. Whereas, the catalysts prepared with en/Co molar ratios of 1 or 3.75 showed lower activities due to their strong interactions between cobalt and silica.

ACKNOWLEDGMENTS

This work was supported by the Natural Science Foundation of China (Contract Nos. 20590361 and 20303026) and The 7th Korea-China Clean Energy Technology Symposium.

REFERENCES

1. H. Schulz, *Appl. Catal. A*, **186**, 3 (1999).
2. S. T. Sie and R. Krishna, *Appl. Catal. A*, **186**, 55 (1999).
3. Z.-W. Liu, X. Li, K. Asami and K. Fujimoto, *Catal. Today*, **104**, 41 (2005).
4. X. Huang, N. O. Elbashir and C. B. Roberts, *Ind. Eng. Chem. Res.*, **43**, 6369 (2004).
5. G. H. Yang, J. J. He, Y. Yoneyama, Y. Z. Han and N. Tsubaki, *Appl. Catal. A*, **329**, 99 (2007).
6. Y. C. Liu, J. G. Chen, K. G. Fang and Y. H. Sun, *Green Chem.*, **9**, 611 (2007).
7. T. Mochizuki, T. Hara, N. Koizumi and M. Yamada, *Appl. Catal. A*, **317**, 97 (2007).
8. B. Dunn, D. Covington, P. Cole, R. Ernst, E. Heider and E. Eyring, *Energy Fuels*, **18**, 1519 (2004).
9. B. Ernst, S. Libs, P. Chaumette and A. Kiennemann, *Appl. Catal. A*, **186**, 145 (1999).
10. Y. L. Wang, B. Hou and Y. H. Sun, *Catal. Comm.*, In Press.
11. F. Dumond, E. Marceau and M. Che, *J. Phys. Chem. C*, **111**, 4780 (2007).
12. B. J. Hathaway and C. E. Lewis, *J. Chem. Soc.*, **A**, 1183 (1969).
13. R. Griesser and H. Sigel, *Inorg. Chem.*, **10**, 2229 (1971).
14. B. D. Cullity, *Elements of X-ray diffraction,* Addison-Wesley, London (1978).
15. K. Pansanga, O. Mekasuwandumrong, J. Panpranot and P. Praserthdam, *Korean J. Chem. Eng.*, **24**, 397 (2007).
16. W. J. Wang and Y. W. Chen, *Appl. Catal.*, **77**, 223 (1991).
17. T. Mochizuki, T. Hara, N. Koizumi and M. Yamada, *Catal. Lett.*, **113**, 165 (2007).
18. R. Trujillano, F. Villain, C. Louis and J. Lambert, *J. Phys. Chem. C*, **111**, 7152 (2007).
19. R. B. Anderson, W. K. Hall, A. Krieg and B. Seligman, *J. Am. Chem. Soc.*, **71**, 183 (1949).